◆ Human Brain Mapping 37:4629–4639 (2016) ◆

Nucleus Accumbens and Caudate Atrophy Predicts Longer Action Selection Times in Young and Old Adults

Matthieu P. Boisgontier,[1]* Peter van Ruitenbeek,[1†] Inge Leunissen,[1] Sima Chalavi,[1] Stefan Sunaert,[2] Oron Levin,[1] and Stephan P. Swinnen[1,3]

[1]*KU Leuven, Movement Control and Neuroplasticity Research Group, Group Biomedical Sciences, Leuven 3001, Belgium*
[2]*KU Leuven, Department of Radiology, University Hospital, Leuven 3001, Belgium*
[3]*KU Leuven, Leuven Research Institute for Neuroscience & Disease (LIND), Leuven 3001, Belgium*

Abstract: There is a convergence in the literature toward a critical role for the basal ganglia in action selection. However, which substructures within the basal ganglia fulfill this role is still unclear. Here we used shape analyses of structural magnetic resonance imaging data to determine the extent to which basal ganglia structures predict performance in easy and complex multilimb reaction-time tasks in young and old adults. Results revealed that inward deformation (i.e., local atrophy) of the nucleus accumbens and caudate were predictive of longer action selection times in complex conditions, but not in easy conditions. Additionally, when assessing the relation between behavioral performance and the shape of the left nucleus accumbens in the two age groups separately, we found a significant performance–structure association in old, but not young adults. This result suggests that the relevance of the nucleus accumbens for the process of action selection increases with age. *Hum Brain Mapp 37:4629–4639, 2016*.

Key words: basal ganglia; humans; motor control

INTRODUCTION

The selection of motor actions is fundamental to the survival of humans and other species. Therefore, action selection likely involves brain structures that were developed in primitive vertebrates and have been conserved throughout evolution (Cisek and Kalaska, 2010). Basal ganglia circuitry has been shown to be present even in the most primitive vertebrates (Grillner et al., 2013; Stephenson-Jones et al., 2011). Furthermore, basal ganglia act as a funnel (Bar-Gad et al., 2003; Mink, 1996), receiving input from a broad range of brain areas, and projecting directly to the brainstem (Rolland et al., 2011) and through the thalamus to the cerebral cortex, implicating both motor and cognitive functions (Behrens et al., 2003; Middleton and Strick, 2000). Furthermore, there is a convergence toward a critical role for basal ganglia in action selection that is

MPB and PVR contributed equally to this work.

Contract grant sponsor: Research Foundation—Flanders (FWO); Contract grant number: 1504015N; 1514115N; G0721.12; G0708.14; Contract grant sponsor: Belgian Science Policy Office; Contract grant number: P7/11; Contract grant sponsor: KU Leuven Research Fund; Contract grant number: C16/15/070

*Correspondence to: Matthieu P. Boisgontier. E-mail: matthieu.boisgontier@faber.kuleuven.be

Received for publication 11 March 2016; Revised 30 June 2016; Accepted 22 July 2016.

DOI: 10.1002/hbm.23333

Published online 1 September 2016 in Wiley Online Library (wileyonlinelibrary.com).

supported by computational models (Eliasmith et al., 2012; Gurney et al., 2001). However, which substructure within the basal ganglia is most predictive for action selection remains unclear.

A measure that has been used to infer the neural processes underlying action control is the actual time taken to process information (Jensen, 2006). Specifically, it has been suggested that subtracting reaction time (RT) in a single task from RT in a multiple-choice condition reflects processes related to action selection (Donders, 1969). However, recent studies demonstrated that this also reflects action preparation (Bastian et al., 2003; Maslovat et al., 2014), and therefore did not sufficiently isolate the selection process. In a recent study, we investigated the complexity of action selection in young adults using the subtraction method with different task variants to isolate the action selection component (Boisgontier et al., 2014). Specifically, the number of limbs that could be moved was identical ($n = 4$) across trials, thereby controlling for the potential effect of action preparation. As a consequence, differences in performance only resulted from differences in action selection processes. Results of the choice—single RT subtraction—revealed that selecting 2 diagonal (e.g., left hand and right foot) and 3 limbs was more complex than selecting 1, 2 ipsilateral, 2 homologous, or 4 limbs (Boisgontier et al., 2014). This new subtraction method may be very useful for studying the involvement of brain structures underlying action selection.

Additionally, studying a motor system that exhibits deficits as a result of aging (Seidler et al., 2010) may be more sensitive to changes in task demands, due to changes in brain structures that are critical for action selection. On a behavioral level, aging has shown to impact both simple and choice RT (Spirduso, 1975) and to increase intraindividual variability in choice RT conditions (Dykiert et al., 2012). Furthermore, the effect of age on RT performance increases with task complexity, suggesting an age $\times$ task complexity interaction effect (Hale et al., 1987). Therefore, aging may interact with the coordination effect we reported earlier. However, the speed/accuracy tradeoff is known to shift toward accuracy in old adults (Starns and Ratcliff, 2010). The interaction between age and complexity may be better reported by RT than error data. On a neurobiological level, Serbruyns et al. (2015) have shown an age-related volumetric decline in the putamen, pallidum, and caudate. What is currently unknown is the extent to which these age-related declines impact regions associated with action selection performance.

To investigate brain correlates of action selection in young and old adults, we used magnetic resonance imaging in association with a multilimb RT task (performed outside the scanner) with a specific emphasis on responses with 2 diagonal and 3 limbs, as these conditions are particularly complex (Boisgontier et al., 2014; Leenus et al., 2015). Specifically, we used statistical shape analysis to investigate whether the shapes (e.g., local structural volume) of specific basal ganglia structures[1], including the putamen, caudate, pallidum, and nucleus accumbens, are predictive of action selection performance, and whether such predictions are dependent on age and the level of task complexity. We hypothesized that (i) the effect of age on RT performance is higher in the most complex conditions, (ii) this effect of age is better evidenced by RT than error rates, (iii) local atrophy of basal ganglia is predictive of action selection taking longer, and (iv) aging alters the relative contribution of these structures to behavioral performance.

MATERIALS AND METHODS

Participants

Thirty-five young (22 ± 3 years; 15 women) and thirty old (70 ± 6 years; 14 women) healthy volunteers participated in this study. All participants were right-handed according to the Edinburgh Handedness Inventory (Oldfield, 1971). The average lateralization quotient was similar between the young and old adults ($+90 \pm 15$ vs $+92 \pm 14$, respectively, with a $+100$ score representing extreme right-hand preference and a -100 score representing extreme left-hand preference). All participants had normal or corrected-to-normal vision, and none reported neurological, psychiatric, cardiovascular, or neuromuscular disorders. Old participants were screened for cognitive impairment with the Montreal Cognitive Assessment test using the standard cutoff score of 26 (Nasreddine et al., 2005). All participants gave their written informed consent, and procedures were performed according to guidelines established by the ethics committee for biomedical research at the KU Leuven, and in accordance with the WMA International Code of Medical Ethics (World Medical Association Inc., 1964).

Multilimb Reaction-Time Task

RT was assessed with the multilimb reaction-time task (Boisgontier et al., 2014). Participants were seated in front of a PC screen, with their forearms resting on a table and their fingers and forefeet on tablets with capacitive proximity switches (Fig. 1A; Pepperl Fuchs CBN5-F46-E2, sampling frequency: 1000 Hz). Four squares representing the four limb segments were presented on the PC screen. Mapping of the stimuli was maximally congruent relative to the effectors, i.e., the right and left upper squares represent the right and left hands, whereas the right and left lower squares represent the right and left feet, respectively. Once all 4 limb segments had contacted the tablets, some of the squares on the PC screen turned blue. In response to this stimulus, participants had to release

[1]The thalamus was also tested and did not show any significant result.

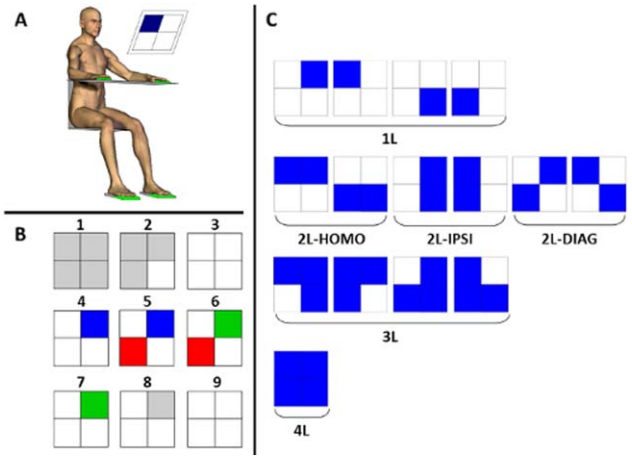

Figure 1.

Multilimb reaction-time task setup. **(A)** Participant setup. Participants were seated in front of a PC screen, their forearms resting on a table and their fingers and forefeet on tablets with capacitive proximity switches (in green). **(B)** Example of a trial sequence represented on the PC screen. The right and left upper squares represent the right and left hands, respectively, whereas the right and left lower squares represent the right and left feet, respectively. (1) Squares are grey when limbs are not in contact with the tablets. (2) The squares turn white as soon as a limb contacts the corresponding tablet. (3) A trial starts as soon as all limbs are in contact with the tablets. (4) When a square on the PC screen turns blue, this is the stimulus for the participant to release contact with the corresponding tablet as quickly as possible. (5) If the participant lifts the incorrect limb(s), the corresponding square(s) turn(s) red. (6) If he lifts the correct limb(s), the corresponding square(s) turn(s) green. (7) A trial is not validated until the response is fully correct, i.e., without any red squares on the screen. (8) As soon as the trial is validated, the green squares turn back to grey. (9) The participant has to reposition all limb segments on the tablets to start a new trial. **(C)**. Coordination modes and clusters. The 15 possible coordination modes were grouped according to 5 clusters (1L, 2L-HOMO, 2L-IPSI, 2L-DIAG, 3L, 4L) based on the number of limbs to be recruited (1, 2, 3, or 4) and limb configuration. Abbreviations: L = limb; DIAG = diagonal; IPSI = ipsilateral; HOMO = homologous. [Color figure can be viewed at wileyonlinelibrary.com]

contact with the corresponding tablets as quickly as possible by simultaneously lifting the corresponding limb segment(s). The specific sequence for each trial was the following (Fig. 1B): Squares are grey when limbs are not in contact with the tablets. They turn white as soon as a limb contacts the corresponding tablet. A trial starts as soon as the four limbs are in contact with the tablets. When one or more squares turn(s) blue, this is the stimulus for the participant to release contact with the corresponding tablet(s) as quickly as possible. If the participant lifts the incorrect limb(s), the corresponding square(s) turn(s) red. If the participant lifts the correct limb(s), the corresponding square(s) turn(s) green. A trial is not validated until the response is fully correct, i.e., without any red squares on the screen. As soon as the trial is validated, the green squares turn back to grey. Then, the participant has to reposition all limb segments on the tablets to start a new trial. All 15 possible coordination modes were tested and arranged in 6 coordination clusters (Fig. 1C) composed of 1-limb coordination modes (1L), 2-homologous upper/lower-limb coordination modes (2L-HOMO), 2-ipsilateral right/left-limb coordination modes (2L-IPSI), 2-diagonal limb coordination modes (2L-DIAG), 3-limb coordination modes (3L), and a 4-limb coordination mode (4L).

The experimental design was composed of two sessions divided by a 5 min break. Each session consisted of two blocks. One block was composed of randomized 5-trial runs of each of the 15 coordination modes. Before each run, the participant viewed a printed copy of the figure that would appear on the screen for the subsequent 5-trial run, thereby removing any choice from the process. This first block measured simple RT. The second block consisted in performing 75 trials (5 trials $\times$ 15 coordination modes) in randomized order, thereby including a choice in the process. This second block measured choice RT. In total, each participant performed 300 trials.

Behavioral Data Analyses

RT was defined as the time interval between the onset of the visual stimulus and the time the participant released all the limbs corresponding to the screen stimulus. RT was averaged for each of the 15 coordination modes in the simple and choice RT blocks. To focus on the cognitive processes involved in motor choice, normalized RT were computed by subtracting the simple RT values from the choice RT values. This was considered our distinct measurement of action selection, free of confounds.

A response was considered as an error when the participant released an incorrect limb. The number of errors was averaged across all trials of a given condition (i.e., number of errors/number of trials) and multiplied by 100 to be expressed as a percentage. Error rates were normalized by subtracting the simple RT values from choice RT condition values. To make the error comparisons meaningful among conditions involving a different number of potential locations of error (i.e., the 1L condition has three potential error locations because 3 limbs can be moved incorrectly, while the 3L condition only has one), normalized error rates in conditions involving 1, 2, and 3 limbs were divided by 3, 2, and 1, respectively.

Image Acquisition

Structural images of the brain were collected using a 3 T Philips Achieva magnetic resonance scanner (Philips Healthcare, Best, The Netherlands) and a 32-channel head

coil. Images were acquired using a T1-weighted, high-esolution, magnetization-prepared rapid gradient echo (MPRAGE) sequence. The sequence consisted of a TR = 9.7 ms, TE = 4.6 ms, and a 8° flip angle, which resulted in 230 sagittal slices with a voxel size of 0.98 × 0.98 × 1 mm^3 in a field of view of 384 × 384 mm.

Image Processing

Before entering the analysis, all images were manually inspected for the presence of anatomical abnormalities or MR artefacts using xjview software in MATLAB R2011a (The MathWorks Inc., Natick, MA, 2011). Next, subdivisions of the basal ganglia (bilateral nucleus accumbens, caudate, pallidum, and putamen) were segmented from the T1 weighted images using FMRIB's Integrated Registration Segmentation Toolkit (FSL FIRST; http://fsl.fmrib.ox.ac.uk/fsl/fslwiki/FIRST; Patenaude et al., 2011) in FSL version 5.0.8. (Jenkinson et al., 2012; Smith et al., 2004; Woolrich et al., 2009). FSL FIRST is an active appearance model approach based on a Bayesian framework segmenting subcortical structures. The active appearance model approach models the distribution of an anatomical point across participants as well as incorporating image intensity information. This allows using probability relationships between shapes of different structures, and between the shape of a structure and image intensity. Furthermore, using a deformable model limits topology of the structures and maintains point correspondence. Finally, the approach is not dependent on tissue classification, which can be problematic for subcortical regions and does not depend on arbitrary smoothing parameters (Patenaude et al., 2011).

The models used are based on a training set of 336 manually labeled anatomical images provided by the Center for Morphometric Analysis (CMA), MGH Boston. The 336 images were collected from a variety of people including old adults, making it representative of our participant sample. The model fitting results in a deformable mesh for each structure, consisting of a set of triangles of which the apex of the adjoining triangles is called a vertex. The meshes were reconstructed in model space (i.e., MNI space) and pose (global rotation and translation) was removed from the meshes by a rigid alignment with 6 degrees of freedom and boundary correction was applied. Segmentations were visually inspected for all participants in sagittal, coronal, and axial views using the FSLVIEW toolbox.

Subcortical Grey Matter Vertex Analyses

Differences in the shape of the meshes, i.e., subcortical structure, represent deformations that may be indicative of individual differences (e.g., age-related local volumetric increases or decreases). Currently, vertex analysis (FSL) is capable of indicating the exact (subregional) location of the relation between grey matter structure and performance. FSL FIRST shape analyses (Patenaude et al., 2011) restricts topology of the structures and preserves interparticipant vertex correspondence, enabling a vertex-wise comparison across individuals or between groups. Differences in shape are quantified using the *first_utils* command in (FSL), which projects vertex locations from each participant onto the surface normal vector (i.e., perpendicular to the tangent plane to the surface and outward pointing) of the average shape of a participant sample. These vertices represent the signed, perpendicular distance from the average surface. Negative values reflect inward deformation of the vertices (i.e., local atrophy) and positive values reflect outward deformation (i.e., local expansion) of the vertices.

Statistical Analyses

Reaction time and errors

To test the cognitive cost associated with a given coordination cluster in young and old adults, normalized RT measures were modeled in Statistica using a 2 × 6 ANOVA with age (young vs old adults) as the between-participant factor and coordination (1L, 2L-HOMO, 2L-IPSI, 2L-DIAG, 3L, and 4L) as the within-participant factor. The 4L coordination cluster always resulted in an absence of error as all limbs had to be recruited. Therefore, normalized error rates were analyzed using a 2 × 5 (age × coordination) ANOVA with repeated measures on the last factor.

For all statistical analyses, the level of significance was set at $P < 0.05$, two-sided. P values of ANOVAs were corrected for sphericity (corr. P) using the Greenhouse-Geisser method when Mauchly's test was significant. To stabilize the variance of the measurements and make the analysis more valid, error rates were transformed using the $(x + 0.5)^{1/2}$ transformation (Bartlett, 1947). When ANOVAs revealed significant effects, post-hoc tests (Tukey HSD, which corrects for multiple comparisons) were conducted to identify the loci of these effects. Partial eta squared ($\eta^2 P$) were reported to indicate small ($\geq$0.01), medium ($\geq$0.06), and large ($\geq$0.14) effect sizes (Sink and Stroh, 2006).

Imaging analyses

For imaging analyses, simple RT, normalized RT, and normalized error rates for each age group in the six task conditions were demeaned and used as predictors in eight regression models predicting subcortical shape of a given structure. Specifically, our analyses tested all basal ganglia structures currently implemented in FSL: left and right nucleus accumbens, caudate, pallidum, and putamen (but not subthalamic nuclei). Total intracranial volume (TIV) was calculated using SPM8 (Ridgway et al., 2011) and used as a covariate controlling for brain size. The focus of

this article was on the association between the shapes of subcortical structures and behavioral performance in easy (1L, 2L-HOMO, 2L-IPSI, 4L) and complex task conditions (2L-DIAG and 3L). For each structure, the two statistical models of interest predicting structural shape were defined as the RT from the easy or complex task conditions as predictor of interest and TIV as predictor of no interest. In addition, given the sexual dimorphism of at least some of the subcortical structures (Rijpkema et al., 2012), gender was also added as a predictor of no interest. A subsequent whole-group negative association between behavioral (i.e., simple RT, normalized RT, and error rates) and brain measures (i.e., signed distance from the average shape of a given structure for each vertex) was further investigated. Structures showing such associations were tested for age-related differences in shape (i.e., deformation) to determine whether age-related differences drove the behavior–brain association. Next, associations between shape and performance were analyzed per age group to determine if one or both age groups determined the whole group result. Models were calculated using the "randomize" procedure in FSL, which is a distribution-free permutation method, using 5000 iterations. Results were regarded as significant at $P < 0.05$ level, with Threshold-Free Cluster Enhancement correction for multiple comparisons (Smith and Nichols, 2009).

Linear mixed models

Finally, to strengthen the validity and specificity of our results, the sum of the significant vertices of the basal ganglia substructures (bilateral nucleus accumbens and caudate, and right pallidum) for each structure and participant were used in linear mixed models to reveal the extent to which these structures predict action selection. Linear mixed models take into account the sampling variability of both the participants and conditions, thereby limiting a large inflation of false positives, whereas traditional analyses of variance disregard such sampling variability (Boisgontier and Cheval, 2016). Moreover, linear mixed models avoid information loss due to averaging over observations, as each single trial is taken into account in the model. Here, the linear mixed model also allowed including all the tested structures in a single model as predictors of RT performance, which was not possible with the vertex analysis. Specifically, an exploratory linear mixed model with choice RT as a dependent variable, the 5 structures as predictors, and simple RT as a covariate (mean of each condition for each subject) was used to define which interactions (structure × complexity) should be tested. The main model was then built, including the structures tested in the exploratory model, the interactions between the structures that were predictive of choice RT in the exploratory model and complexity (easy vs complex). This main model controlled for the effect of age (young vs old adults), gender (males vs females), simple RT, error (vs no error), session (1 vs 2), trial (1 to 75), and total intracranial volume. These models specified participants ($n = 65$) and conditions ($n = 15$) as random factors and were built using the R language lmerTest package, version 2.0–30 (http://www.r-project.org/). The continuous variables were scaled and centered on zero. Predictors were checked for the absence of multicollinearity and showed variance inflation factors below five (Hair et al., 1995).

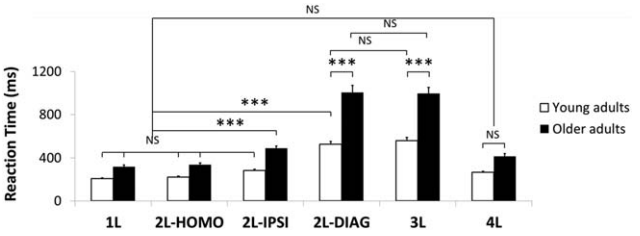

Figure 2.
Normalized reaction time in the six coordination modes in young (white bars) and old adults (black bars). ***$P < 0.001$; NS, nonsignificant.

RESULTS

Multilimb Reaction-Time Task

With regard to normalized RT, the two-way ANOVA demonstrated main effects of age [$F(1,63) = 75.05$; $P < 0.001$; $\eta^2_P = 0.54$], and coordination [$F(5,315) = 199.59$; $P < 0.001$; $\eta^2_P = 0.76$], and an interaction effect of age × coordination [$F(5,315) = 22.93$; $P < 0.001$; $\eta^2_P = 0.27$]. Post-hoc analyses revealed that RT were the longest in the 2L-DIAG and 3L conditions (735 and 757 ms respectively; ps < 0.001), and the shortest in the 1L, 2L-HOMO, and 4L conditions (256 ms, 274 ms, and 318 ms, respectively; Fig. 2). RT in the 2L-IPSI (377 ms) was longer than 1L and 2L-HOMO but shorter than the 2L-DIAG and 3L conditions. Furthermore, old adults showed significantly longer RT in the 2L-IPSI, 2L-DIAG, and 3L conditions as compared to the young adults (486 vs 284 ms, 978 vs 527 ms, and 985 vs 562 ms, respectively).

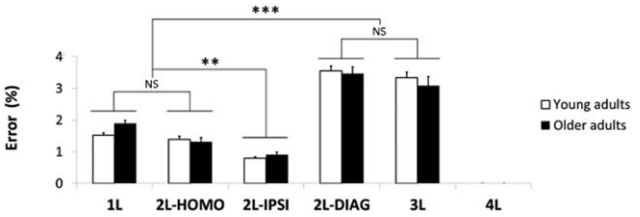

Figure 3.
Normalized error rate in the six coordination modes in young (white bars) and old adults (black bars). ***$P < 0.001$; **$P < 0.01$; NS, nonsignificant.

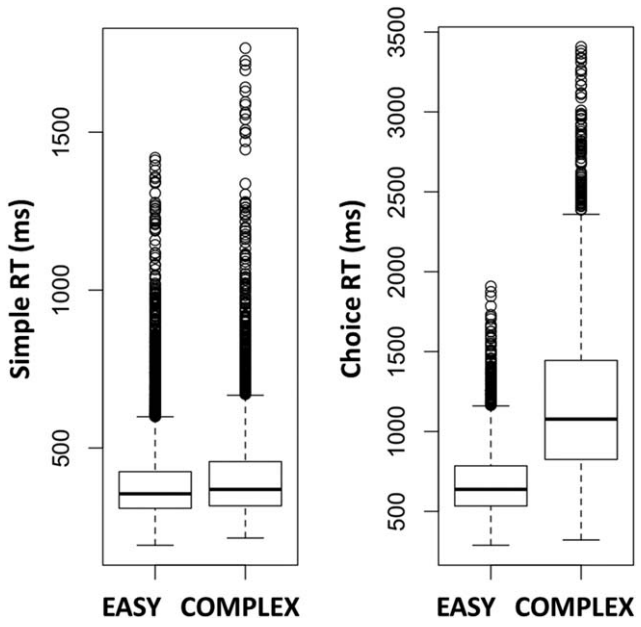

Figure 4.
Raw simple and choice reaction time (RT) in the easy (1L, 2L-HOMO, 2L-IPSI, 4L) and complex conditions (2L-DIAG and 3L).

With regard to normalized error rates, the two-way ANOVA demonstrated a main effect of coordination [$F(4,252) = 125.62$; $P < 0.001$; $\eta^2_P = 0.67$]. Post-hoc analyses revealed that error rates were the highest in the 2L-DIAG and 3L condition (3.5 and 3.2%, respectively; ps < 0.001) and the lowest in the 2L-IPSI condition (0.8%; $P < 0.006$) (Fig. 3). In contrast, the main effect of age [$F(1,63) < 0.01$; $P = 0.964$; $\eta^2_P < 0.01$] and the interaction effect [$F(4,252) = 1.31$; $P = 0.273$; $\eta^2_P = 0.02$] were not significant.

Basal Ganglia Structures

As RTs were the shortest in the 1L, 2L-HOMO, and 4L conditions and the longest in the 2L-DIAG and 3L conditions, brain structure analyses were performed on easy (1L, 2L-HOMO, 2L-IPSI, 4L) and complex task conditions (2L-DIAG and 3L). Raw data of simple and choice RT in these easy and complex conditions are reported in Figure 4. Analyses of the relation between performance in the easy task conditions (1L, 2L-HOMO, 2L-IPSI, 4L) and the shapes of subcortical structures across the whole group did not result in any significance. Conversely, analyses of the relation between performance in the most complex task conditions (2L-DIAG and 3L) and the shapes of subcortical structures across the whole group resulted in significant associations. Specifically, longer normalized RT during the most complex conditions was associated with inward deformations of the mostly lateral and inferior medial right pallidum. Also, associations were established with medial parts of the left and right caudate. Inward deformations of the posterior, anterior, and medial part of the left nucleus accumbens, and almost the entire surface of the right nucleus accumbens (Fig. 5, in red-yellow) were also associated with longer RT. No associations were detected with the putamen. Finally, the same vertex analyses, but with simple RT (and gender and TIV) as predicting variables, did not show any significant results, thereby strengthening the specificity of the previous results.

Age-related inward deformation was observed in large parts of the bilateral pallidum, caudate, and accumbens (Fig. 6, in green-blue). In addition, these areas demonstrating age-related decline showed substantial overlap with areas associated with RT performance (Figs. 5 and 6). To quantify this overlap, we calculated the percentage of the vertices associated with action selection performance that were also associated with the age of the participant. Results showed that 87.6% of the area of the right pallidum was associated with both performance and age. There was a 100% overlap for the left and right caudate, and respectively 100% and 97.4% for the left and right nucleus accumbens.

Dividing the total sample into young and old adult subgroups resulted in a significant performance–structure association in the posterior and anterior parts of left

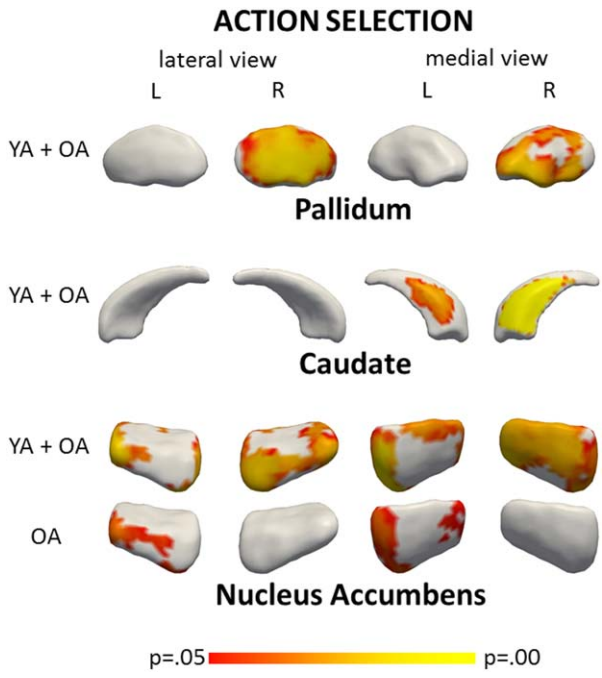

Figure 5.
Association between performance in most complex task conditions (normalized reaction time in 2L-DIAG and 3-L) and inward deformation (i.e., local atrophy) of the pallidum, caudate, and nucleus accumbens in young and old adults. YA, young adults; OA, old adults; L, left; R, right. [Color figure can be viewed at wileyonlinelibrary.com]

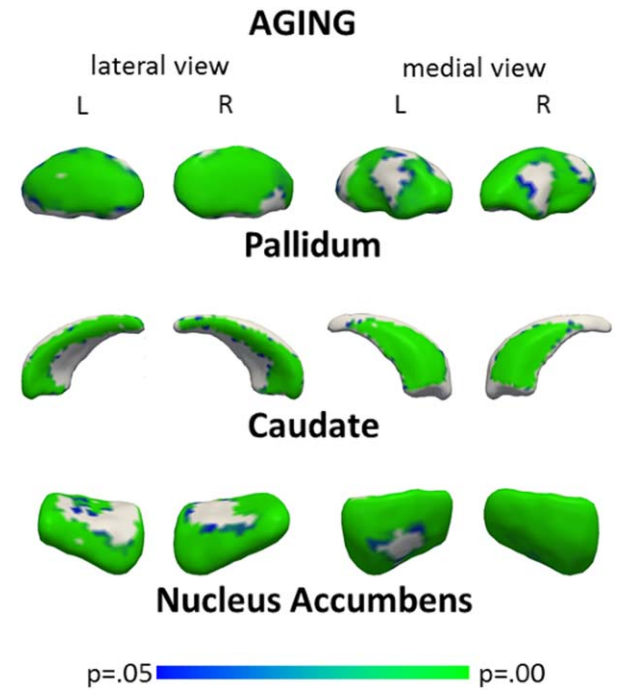

Figure 6.

Association between age (young vs old adults) and inward deformation (i.e., local atrophy) of the pallidum, caudate, and nucleus accumbens. L, left; R, right. [Color figure can be viewed at wileyonlinelibrary.com]

nucleus accumbens in old, but not young adults (Fig. 5). The contrasts testing normalized error rates as predictors for subcortical shapes were not significant.

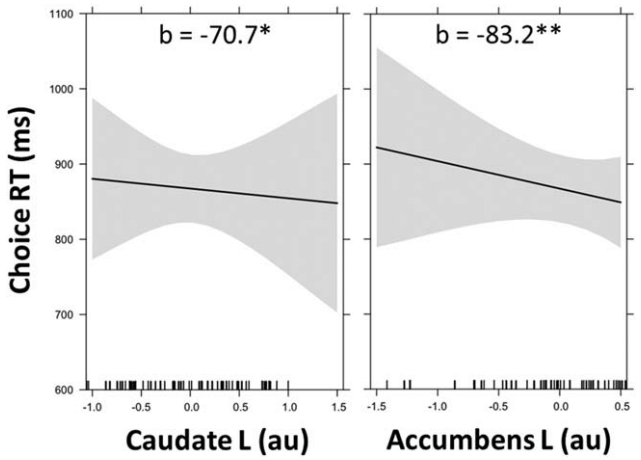

Figure 7.

Fixed effects and the 95% confidence interval of the mean of the vertex values of the left caudate and left accumbens on choice reaction time (RT). These effects were significant while controlling for all the other effects reported in Table I, including simple reaction time and age group.

Results of the exploratory linear mixed model showed a significant fixed effect of simple RT ($b = 66.0$, $P < 0.001$), left caudate ($b = -95.2$, $P < 0.001$), and left nucleus accumbens ($b = -55.1$, $P = 0.042$). The fixed effects of the right pallidum ($b = -0.8$, $P = 0.972$), right caudate ($b = 24.7$, $P = 0.105$), and right accumbens were not significant ($b = -0.24$, $P = 0.993$).

Results of the main linear mixed model (Table I) showed a significant interaction between the effect of complexity and the effects of the left caudate ($b = 98.4$, $P < 0.001$) and left nucleus accumbens ($b = 96.6$, $P < 0.001$), and revealed that these structures predicted choice RT in the complex ($P < 0.016$), but not easy conditions ($P > 0.330$). Importantly, these effects of the left caudate ($b = -70.7$, $P = 0.016$; Fig. 7) and left nucleus accumbens ($b = -83.2$, $P = 0.001$; Fig. 7) in the complex conditions were significant while controlling for the effect of simple choice RT ($b = 22.8$, $P < 0.001$), thereby allowing these effects to be predictive of the action selection process. Furthermore, these effects were significant irrespective of age group ($b = 326.7$, $P < 0.001$), gender ($b = -15.9$, $P = 0.746$), the number of failed trials ($b = 288.8$, $P = 0.083$), the practice effect across sessions ($b = -63.0$, $P < 0.001$) and trial ($b = -0.4$, $P < 0.001$), and total intracranial volume ($b = -8.8$, $P = 0.740$). In sum, the atrophy of the left caudate and left nucleus accumbens was the only basal ganglia substructures predicting action selection in the complex conditions.

DISCUSSION

Here we investigated whether the shape of specific basal ganglia structures was associated with action selection performance in a multilimb RT task, and whether such predictions are dependent on age and the level of task complexity. As expected on the basis of the study by Boisgontier et al. (2014), behavioral results demonstrated the highest normalized RT and error rates in the 2L-DIAG and 3L conditions for both young and old adults. Furthermore, the difference in performance between young and old adults, as assessed with normalized RT, was the largest in these two task conditions. These results suggest specific age-related impairment in processes underlying performance during these conditions. Imaging analyses and linear mixed models revealed that local atrophy of the left caudate and left nucleus accumbens were predictive of performance in the most complex task conditions, but not in the easier conditions. This result indicates that the central processing that dissociates the 2L-DIAG and 3L conditions from the other conditions is related to caudate and nucleus accumbens grey matter.

Action Selection in Young and Old Adults

To be able to interpret the results of this study, we first need to account for the mechanisms that dissociate the two most complex task conditions (2L-DIAG and 3L) from

TABLE I. Predictors of the choice reaction time (RT)

	Easy			Complex		
Fixed Effects	*b*	SE	*P*	*b*	SE	*P*
Intercept	5.869×10^{2}	4.379×10^{1}	<0.001***	1.095×10^{3}	4.650×10^{1}	<0.001***
Young vs Old adult	3.267×10^{2}	6.282×10^{1}	<0.001***	3.267×10^{2}	6.282×10^{1}	<0.001***
Male vs female	-1.590×10^{1}	4.878×10^{1}	0.746	-1.590×10^{1}	4.878×10^{1}	0.746
Simple reaction time	2.282×10^{1}	4.736×10^{0}	<0.001***	2.282×10^{1}	4.736×10^{0}	<0.001***
Error (0 vs 1)	2.888×10^{2}	1.663×10^{2}	0.083	2.888×10^{2}	1.663×10^{2}	0.083
Session (1 vs 2)	-6.296×10^{1}	5.010×10^{0}	<0.001***	-6.296×10^{1}	5.010×10^{0}	<0.001***
Trial (1–75)	-3.940×10^{-1}	1.163×10^{-1}	<0.001***	-3.940×10^{-1}	1.163×10^{-1}	<0.001***
Complexity	5.086×10^{2}	3.533×10^{1}	<0.001***	-5.086×10^{2}	3.533×10^{1}	<0.001***
Total intracranial volume	-8.764×10^{0}	2.633×10^{1}	0.740	-8.764×10^{0}	2.633×10^{1}	0.740
Caudate R	1.633×10^{1}	1.405×10^{1}	0.248	1.633×10^{1}	1.405×10^{1}	0.248
Accumbens R	1.532×10^{1}	2.438×10^{1}	0.532	1.532×10^{1}	2.438×10^{1}	0.532
Pallidum R	1.738×10^{0}	2.214×10^{1}	0.938	1.738×10^{0}	2.214×10^{1}	0.938
Caudate L	2.772×10^{1}	2.826×10^{1}	0.330	-7.068×10^{1}	2.847×10^{1}	0.016*
Accumbens L	1.347×10^{1}	2.485×10^{1}	0.590	-8.317×10^{1}	2.510×10^{1}	0.001**
Caudate L × complexity	9.664×10^{1}	6.266×10^{0}	<0.001***	9.664×10^{1}	6.266×10^{0}	<0.001***
Accumbens L × complexity	9.841×10^{1}	6.218×10^{0}	<0.001***	9.841×10^{1}	6.218×10^{0}	<0.001***
Random effects	σ^2					
Participant						
Intercept	1.426×10^{4}					
Condition						
Intercept	4.369×10^{3}					
Residual		5.476×10^{4}				

L, left; R, right; $P < 0.1$; *$P < 0.05$; **$P < 0.01$; ***$P < 0.001$.

the others. On an information processing level, Boisgontier et al. (2014) have studied the principles that govern information processing during choice RT task performance, and constructed a model in which two principles determine RT. First, the recruitment principle states that response complexity increases with the number of effectors to be moved. Second, the selection principle states that moving a particular combination of effectors (e.g., 2 limbs located diagonally vs ipsilaterally) determines response complexity. While performance in choice RT tasks is highly dependent on both of these principles, performance in simple RT tasks is mainly dependent on the recruitment principle. Therefore, by normalizing the RT data (i.e., choice RT − simple RT), a clean measure of the time needed for limb selection can be obtained. The longer normalized RT, as observed in our study during 2L-DIAG and 3L task conditions, can therefore be explained by increased complexity in the specific process of limb selection and this should be considered against the backdrop of specific (neural) coupling effects among the 4 effectors. More specifically, coupling is strongest between the homologous effectors, followed by ipsilateral and diagonal effectors. This implies that selection of one hand may also facilitate selection of the contralateral hand unless this is actively suppressed, and the same applies for the feet (Boisgontier et al. 2014). This is actually supported by transcranial magnetic stimulation work in a choice RT task, showing that selection of 1 limb is associated with active inhibition of the homologous limb (Cuypers et al., 2013), highlighting homologous bimanual movement as being the default movement. Additionally, the level of inhibition of cortical motor pathways in cyclical movements has shown to be higher between ipsilateral, relative to diagonal limbs (Fujiyama et al., 2009). Old adults are disproportionally impaired during these task conditions, as suggested by the normalized RT data. This impairment supports previous studies highlighting an age-related decline in inhibitory pathways (Levin et al., 2014), especially that associated with diagonal movements (Fujiyama et al., 2012). Taken together, these results suggest that brain structures associated with action selection (as determined in our RT task) are also involved in the regulation of inhibitory pathways.

It is important to note that, as compared to RT, aging did not impact normalized error rates. The absence of disproportionate error rates is consistent with performance strategies known in old adults. Being aware of their impairment, old adults adapt by slowing down the response time to emphasize response accuracy. In other words, the speed/accuracy tradeoff is shifted toward accuracy and this is a remarkable strategic phenomenon in the aging system (Starns and Ratcliff, 2010). Therefore, the impact of age on action selection was only revealed through RT and not error rate.

Nucleus Accumbens

So far, the nucleus accumbens, often referred to as the ventral striatum, has widely been considered as a critical structure within the reward circuitry (Ikemoto and Panksepp, 1999). Specifically, the nucleus accumbens is activated when successfully choosing between a variety of nonmotor responses (e.g., Botvinick et al. 2009, Kuhnen and Knutson 2005). However, increasingly attention is turning to the potential role of the nucleus accumbens in a diversity of behavioral functions, including motor control and learning (Floresco, 2015; Salamone et al., 2005; Sawada et al., 2015). Specifically, administration of dopamine/norepinephrine agonist in the core of the nucleus accumbens results in premature responses in a choice RT task (Economidou et al., 2012). Experimentally impaired nucleus accumbens functioning shows large effects on RT performance when there is ambiguity in the correct choice of response (Christakou et al. 2004, Pezze et al. 2007). Taken together, reward and RT studies suggest that the nucleus accumbens is involved in both approach and avoidance behavior at the psychological and at the motor level. Our results clearly supported this view of the nucleus accumbens being critical in action selection, especially in old adults. Therefore, the age-related difference in normalized RTs could be accounted for by the possible age-related structural alteration of the nucleus accumbens.

Caudate

The association between performance and the caudate structure was significant only in the more complex conditions of our multilimb RT task. This is consistent with results of a study using the Tower of London task and showing that the activity of the caudate was correlated with task complexity (Dagher et al., 1999). Other studies showed that the caudate is critical in performing automatic tasks and adapting fast responses (Iaria et al., 2003; Poldrack et al., 2001). Here, the ability to link perceptual information or input with motor output commands in an automatic manner indeed likely mainly determined performance in the complex conditions.

Pallidum

In the literature, blockade of the pallidum has been shown to increase RT in monkeys (Kato and Kimura, 1992), whereas other studies did not show any involvement of the pallidum in RT (Amato et al., 1978; Horak and Anderson, 1984; Mink and Thach, 1991). Accordingly, the impact of the pallidum on RT was unclear as was the effect of task complexity. Results of the shape analysis suggested that pallidal integrity was associated with performance during complex, but not during easy task conditions. However, the linear mixed model revealed that when all the basal ganglia substructures are taken into account, the pallidum does not predict action selection. We also showed that the association between performance and pallidum structure was not affected by age. Therefore, the age-related difference in normalized RTs could not be explained by the possible age-related structural alteration of the pallidum.

CONCLUSION

On a behavioral level, we showed that (i) age impacts action selection in demanding task conditions such as moving 2 diagonally located limbs or 3 limbs, and (ii) this age-related impairment is evidenced by RT, but not error rates. On a neurobiological level, we showed that (iii) local atrophy of the caudate and nucleus accumbens are associated with longer action selection times and (iv) the action selection performance in old adults is more tightly linked to local atrophy of the left nucleus accumbens than in young adults. This latter result corroborates emerging evidence suggesting that the nucleus accumbens is particularly relevant for the process of action selection.

AUTHOR CONTRIBUTIONS

Experimental conception and design: MPB and SPS. Experimental conduct: MPB and OL. Analysis of reaction-time data: MPB. Analysis of imaging data: MPB and PVR. Statistical analysis: MPB. First draft preparation: MPB and PVR. Manuscript preparation: MPB, PVR, IL, SC, SS, OL, and SPS.

CONFLICT OF INTEREST

The authors declare no conflict of interest.

REFERENCES

Amato G, Trouche E, Beaubaton D, Grangetto A (1978): The role of internal pallidal segment on the initiation of a goal directed movement. Neurosci Lett 9:159–163.

Bar-Gad I, Morris G, Bergman H (2003): Information processing, dimensionality reduction and reinforcement learning in the basal ganglia. Prog Neurobiol 71:439–473.

Bartlett MS (1947): The use of transformations. Biometrics 3:39–52.

Bastian A, Schöner G, Riehle A (2003): Preshaping and continuous evolution of motor cortical representations during movement preparation. Eur J Neurosci 18:2047–2058.

Behrens TE, Johansen-Berg H, Woolrich MW, Smith SM, Wheeler-Kingshott CA, Boulby PA, Barker GJ, Sillery EL, Sheehan K, Ciccarelli O, Thompson AJ, Brady JM, Matthews PM (2003): Non-invasive mapping of connections between human thalamus and cortex using diffusion imaging. Nat Neurosci 6:750–757.

Boisgontier MP, Cheval B (2016): The anova to mixed model transition. Neurosci Biobehav Rev 68:1004–1005.

Boisgontier MP, Wittenberg GF, Fujiyama H, Levin O, Swinnen SP (2014): Complexity of central processing in simple and choice multilimb reaction-time tasks. PLoS ONE 9:e90457.

Botvinick MM, Huffstetler S, McGuire JT (2009): Effort discounting in human nucleus accumbens. Cogn Affect Behav Neurosci 9:16–27.

Cisek P, Kalaska JF (2010): Neural mechanisms for interacting with a world full of action choices. Annu Rev Neurosci 33: 269–298.

Christakou A, Robbins TW, Everitt BJ (2004): Prefrontal cortical-ventral striatal interactions involved in affective modulation of attentional performance: Implications for corticostriatal circuit function. J Neurosci 24:773–780.

Cuypers K, Thijs H, Duque J, Swinnen SP, Levin O, Meesen RL (2013): Age-related differences in corticospinal excitability during a choice reaction time task. Age 35:1705–1719.

Dagher A, Owen AM, Boecker H, Brooks DJ (1999): Mapping the network for planning: A correlational PET activation study with the Tower of London task. Brain 122:1973–1987.

Donders FC (1969): On the speed of mental processes. Acta Psychol 30:412–431.

Dykiert D, Der G, Starr JM, Deary IJ (2012): Age differences in intra-individual variability in simple and choice reaction time: Systematic review and meta-analysis. PLoS ONE 7: e45759.

Economidou D, Theobald DE, Robbins TW, Everitt BJ, Dalley JW (2012): Norepinephrine and dopamine modulate impulsivity on the five-choice serial reaction time task through opponent actions in the shell and core sub-regions of the nucleus accumbens. Neuropsychopharmacology 37:2057–2066.

Eliasmith C, Stewart TC, Choo X, Bekolay T, DeWolf T, Tang Y, Rasmussen D (2012): A large-scale model of the functioning brain. Science 338:1202–1205.

Floresco SB (2015): The nucleus accumbens: An interface between cognition, emotion, and action. Annu Rev Psychol 66:25–52.

Fujiyama H, Garry MI, Levin O, Swinnen SP, Summers JJ (2009): Age-related differences in inhibitory processes during interlimb coordination. Brain Res 1262:38–47.

Fujiyama H, Hinder MR, Schmidt MW, Garry MI, Summers JJ (2012): Age-related differences in corticospinal excitability and inhibition during coordination of upper and lower limbs. Neurobiol Aging 33:1484.e1–1414.

Grillner S, Robertson B, Stephenson-Jones M (2013): The evolutionary origin of the vertebrate basal ganglia and its role in action selection. J Physiol 591:5425–5431.

Gurney K, Prescott TJ, Redgrave P (2001): A computational model of action selection in the basal ganglia. I. A new functional anatomy. Biol Cybern 84:401–410.

Hair JF Jr, Anderson RE, Tatham RL, Black WC. Multivariate data analysis. 3rd ed. New York: Macmillan; 1995.

Hale S, Myerson J, Wagstaff D (1987): General slowing of nonverbal information processing: Evidence for a power law. J Gerontol 42:131–136.

Horak FB, Anderson ME (1984): Influence of globus pallidus on arm movements in monkeys. I. Effects of kainic acid-induced lesions. J Neurophysiol 52:290–304.

Iaria G, Petrides M, Dagher A, Pike B, Bohbot VD (2003): Cognitive strategies dependent on the hippocampus and caudate nucleus in human navigation: Variability and change with practice. J Neurosci 23:5945–5952.

Ikemoto S, Panksepp J (1999): The role of nucleus accumbens dopamine in motivated behavior: A unifying interpretation with special reference to reward-seeking. Brain Res Rev 31:6–41.

Jenkinson M, Beckmann CF, Behrens TE, Woolrich MW, Smith SM (2012): FSL. NeuroImage 62:782–790.

Jensen AR (2006): Clocking the Mind: Mental Chronometry and Individual Differences. Oxford: Elsevier. 287 p.

Kato M, Kimura M (1992): Effects of reversible blockade of basal ganglia on a voluntary arm movement. J Neurophysiol 68:1516–1534.

Kuhnen CM, Knutson B (2005): The neural basis of financial risk taking. Neuron 47:763–770.

Leenus DJ, Cuypers K, Vanvlijmen D, Meesen RL (2015): The effect of anodal transcranial direct current stimulation on multi-limb coordination performance. Neuroscience 290:11–17.

Levin O, Fujiyama H, Boisgontier MP, Swinnen SP, Summers JJ (2014): Aging and motor inhibition: A converging perspective provided by brain stimulation and imaging approaches. Neurosci Biobehav Rev 43:100–117.

Maslovat D, Klapp ST, Jagacinski RJ, Franks IM (2014): Control of response timing occurs during the simple reaction time interval but on-line for choice reaction time. J Exp Psychol Hum Percept Perform 40:2005–2021.

Middleton FA, Strick PL (2000): Basal ganglia and cerebellar loops: Motor and cognitive circuits. Brain Res Rev 31:236–250.

Mink JW (1996): The basal ganglia: Focused selection and inhibition of competing motor programs. Prog Neurobiol 50:381–425.

Mink JW, Thach WT (1991): Basal ganglia motor control. III. Pallidal ablation: Normal reaction time, muscle cocontraction, and slow movement. J Neurophysiol 65:330–351.

Nasreddine ZS, Phillips NA, Bédirian V, Charbonneau S, Whitehead V, Collin I, Cummings JL, Chertkow H (2005): The Montreal Cognitive Assessment, MoCA: A brief screening tool for mild cognitive impairment. J Am Geriatr Soc 53:695–699.

Oldfield RC (1971): The assessment and analysis of handedness: The Edinburgh inventory. Neuropsychologia 9:97–113.

Patenaude B, Smith SM, Kennedy DN, Jenkinson M (2011): A Bayesian model of shape and appearance for subcortical brain segmentation. Neuroimage 56:907–922.

Pezze MA, Dalley JW, Robbins TW (2007): Differential roles of dopamine D1 and D2 receptors in the nucleus accumbens in attentional performance on the five-choice serial reaction time task. Neuropsychopharmacology 32:273–283.

Poldrack RA, Clark J, Pare-Blagoev EJ, Shohamy D, Creso Moyano J, Myers C, Gluck MA (2001): Interactive memory systems in the human brain. Nature 414:546–550.

Ridgway G, Barnes J, Pepple T, Fox N (2011): Estimation of total intracranial volume; a comparison of methods. Alzheimers Dement 7:S62–S63.

Rijpkema M, Everaerd D, van der Pol C, Franke B, Tendolkar I, Fernández G (2012): Normal sexual dimorphism in the human basal ganglia. Hum Brain Mapp 33:1246–1252.

Rolland AS, Karachi C, Muriel MP, Hirsch EC, François C (2011): Internal pallidum and substantia nigra control different parts of the mesopontine reticular formation in primate. Mov Disord 26:1648–1656.

Salamone JD, Correa M, Mingote SM, Weber SM (2005): Beyond the reward hypothesis: Alternative functions of nucleus accumbens dopamine. Curr Opin Pharmacol 5:34–41.

Sawada M, Kato K, Kunieda T, Mikuni N, Miyamoto S, Onoe H, Isa T, Nishimura Y (2015): Function of the nucleus accumbens in motor control during recovery after spinal cord injury. Science 350:98–101.

Serbruyns L, Leunissen I, Huysmans T, Cuypers K, Meesen RL, Van Ruitenbeek P, Sijbers J, Swinnen SP (2015): Subcortical volumetric changes across the adult lifespan: Subregional thalamic atrophy accounts for age-related sensorimotor performance declines. Cortex 65:128–138.

Seidler RD, Bernard JA, Burutolu TB, Fling BW, Gordon MT, Gwin JT, Kwak Y, Lipps DB (2010): Motor control and aging: Links to age-related brain structural, functional, and biochemical effects. Neurosci Biobehav Rev 34:721–733.

Sink CA, Stroh HR (2006): Practical significance: the use of effect sizes in school counseling research. Prof Sch Couns 9:401–411.

Smith SM, Jenkinson M, Woolrich MW, Beckmann CF, Behrens TEJ, Johansen-Berg H, Bannister PR, De Luca M, Drobnjak I, Flitney DE, Niazy R, Saunders J, Vickers J, Zhang Y, De Stefano N, Brady JM, Matthews PM (2004): Advances in functional and structural MR image analysis and implementation as FSL. NeuroImage 23:S208–S219.

Smith SM, Nichols TE (2009): Threshold-free cluster enhancement: Addressing problems of smoothing, threshold dependence and localisation in cluster inference. Neuroimage 44:83–98.

Spirduso WW (1975): Reaction and movement time as a function of age and physical activity level. J Gerontol 30:435–440.

Starns JJ, Ratcliff R (2010): The effects of aging on the speed-accuracy compromise: Boundary optimality in the diffusion model. Psychol Aging 25:377–390.

Stephenson-Jones M, Samuelsson E, Ericsson J, Robertson B, Grillner S (2011): Evolutionary conservation of the basal ganglia as a common vertebrate mechanism for action selection. Curr Biol 21:1081–1091.

Woolrich MW, Jbabdi S, Patenaude B, Chappell M, Makni S, Behrens T, Beckmann C, Jenkinson M, Smith SM (2009): Bayesian analysis of neuroimaging data in FSL. NeuroImage 45:S173–S186.